Research in Pharmaceutical Sciences, April 2025; 20(2): 268-291
Received: 26-04-2023
Peer Reviewed: 06-06-2023
Revised: 22-01-2024
Accepted: 03-02-2024
Published: 31-03-2025

School of Pharmacy & Pharmaceutical Sciences
Isfahan University of Medical Sciences

Original Article

Designing of a novel chimeric antimicrobial peptide against *Acinetobacter baumannii* using three different bioinformatics methods and evaluation of its antimicrobial activity *in vitro*

Yasin Rakhshani[1], Jafar Amani[2,*], Hamideh Mahmoodzadeh Hosseini[2], Seyed Ali Mirhosseini[2], and Fattah Sotoodeh Nejad Nematalahi[1]

[1]Faculty of Converging Sciences and Technologies, Science and Research Branch, Islamic Azad University, Tehran, I.R. Iran.
[2]Applied Microbiology Research Center, Biomedicine Technologies Institute, Baqiyatallah University of Medical Sciences, Tehran, I.R. Iran.

Abstract

Background and purpose: The study aimed to design new chimeric antimicrobial peptides targeting *Acinetobacter baumannii*, a widespread and growing global concern due to antibiotic resistance. Three bioinformatics-based methods were utilized for this purpose.
Experimental approach: To design new chimeric peptides targeting *Acinetobacter baumannii*, a group of peptides were initially selected and divided into two categories based on their scores and performance. The peptides were then combined through 3 methods: 1. combining sequences based on their secondary structure using GOR IV software; 2. grouping only the amino acid sequences involved in the formation of the target peptide helix structure using Accelrys DS visualizer software; and 3. combining the most similar parts of the peptides in terms of amino acid type and order using online AntiBP2 software. The sequence length was optimized, and some amino acids were substituted.
Findings/Results: The M-CIT peptide was selected for synthesis in the first method, but it did not show significant activity against the target bacteria (MIC = 187.5 µM and MBC = 375 µM). In the second method, no suitable score was observed. However, the M-PEX12 peptide was synthesized in the second method, demonstrating antimicrobial activity against *A. baumannii* (MIC = 33.1 µM and MBC = 41.4 µM).
Conclusion and implications: Three methods were evaluated for designing new chimeric peptides, and the third method, which involved modifying the number of amino acids in the parental peptides while maintaining their similarity, was found to be the most suitable.

Keywords: *Acinetobacter baumanni*; Antimicrobial peptide; Drug design; Hybrid peptides; Model membrane; Web servers.

INTRODUCTION

Despite recent advancements, infectious diseases continue to be significant global health challenges, necessitating the development of new antimicrobial agents. Additionally, the emergence of multidrug-resistant and pan-drug-resistant pathogens has presented formidable obstacles in treating infectious diseases, leading to widespread concerns, particularly in intensive care units (ICUs) (1).

Acinetobacter baumannii (*A. baumannii*) is one of the most problematic pathogenic microorganisms that threaten public health, especially in recent years (1,2). *A. baumannii* poses significant challenges in the treatment of hospitalized patients, particularly those in the ICU due to its ability to survive in diverse environmental conditions. This bacterium is recognized for producing pathogenic factors, including biofilms, contributing to its ability to endure dry environmental conditions (3-5).

*Corresponding author: J. Amani
E-mail: jafar.amani@gmail.com
Tel: +98-2182482568, Fax: +98-2188039883

Access this article online

Website: http://rps.mui.ac.ir

DOI: 10.4103/RPS.RPS_70_23

In addition, *A. baumannii* and other strains of *Acinetobacter* exhibit high levels of resistance to almost all known antibiotics, emphasizing the urgent requirement for the development of novel antimicrobial agents (6). Over the past 3 decades, antimicrobial peptides (AMPs) have been extensively studied as potential antimicrobial agents. These natural compounds are found in a variety of organisms and are part of the innate immune system, exhibiting antimicrobial activity (7). Peptides with antimicrobial properties are typically positively charged, while bacterial membranes are negatively charged. This difference in charge results in an electrostatic interaction between the peptide and the bacterial membrane, causing vibrations and changes in the structure of the membrane. AMPs have 2 mechanisms of action. The first mechanism affects the bacterial membrane, resulting in its destruction cytoplasmic leakage, and ultimately bacteria death. The second mechanism includes the inhibition of metabolic pathways such as DNA, RNA, and protein synthesis (8-10). However, despite the benefits, AMPs also have limitations, including instability, immunogenicity, cell toxicity, and high production costs (11).

For nearly 2 decades, modifying the natural sequence of peptides has been considered one of the approaches to developing efficient AMPs. Many studies have found that the natural biological activities of peptides can be modified by creating complex and artificial alterations in amphipathicity, hydrophobicity, net charge, grand average of hydropathy (GRAVY), instability, and Boman index. These changes can significantly reduce the length and number of amino acids used in peptide design, resulting in increased strength and optimal selection against specific pathogens. Additionally, it allows for the production of peptides with lower toxicity and cost (12-14). According to investigations performed on AMPs against sensitive and resistant bacteria such as *S. aureus* and *E. coli* (15), the current study aimed at designing novel chimeric AMPs against *A. baumannii* and evaluating their physicochemical activity and properties *in vitro*.

MATERIALS AND METHODS

Selection of peptides with activity against A. baumannii and analysis of their physicochemical properties

Initially, peptides with inhibitory effects on *A. baumannii* were extracted from the literature. The physicochemical properties of the identified peptide sequences were then determined using the APD3 online software available at https://wangapd3.com/main.php. Peptides with high efficacy against a broad spectrum of targets, low toxicity to eukaryotic cells, low effective concentration, and short effective time were selected as indicator peptides (16-20).

The physicochemical characteristics of the peptides included the following:

1. Number of amino acids: based on comparing the total number of AMPs on the APD3 website, those with 22 - 25 amino acids were the most abundant.

2. Net charge: the net charge was the sum of the charges of each amino acid in the peptide. AMPs typically have a net positive charge, with the most having a net charge ranging from +2 to +9.

3. Isoelectric point (pI): the pH at which a protein or peptide carries no net electrical charge. The pI of AMPs is typically around 10.

4. Aliphatic index: it has been suggested that amino acids such as alanine, isoleucine, leucine, and valine contribute to thermal stability in peptides. The higher the content of the amino acids in a peptide, the more thermally stable it is believed to be.

5. Instability index: the index predicts peptide stability based on the amino acid composition, and a value of less than 40 indicates that the peptide is more stable.

6. Boman index: the index predicts the potential interaction of a peptide with other proteins, focusing on the interaction of peptides with cell membranes. Peptides with a more negative or about zero Boman index are considered more valuable as an AMP.

7. Hydrophobicity index: hydrophobicity is a critical factor in peptide folding and varies depending on the solvent in which the peptide is present. The hydrophobicity index is calculated by summing the hydrophobicity of

each amino acid and dividing it by the total number of amino acids. In the case of AMPs, the hydrophobicity index should be higher than 50%.

8. Grand average of hydropathy (GRAVY): the GRAVY index predicts the hydrophobicity or hydrophilicity peptide. A positive GRAVY value indicates a hydrophobic peptide, while a negative value indicates a hydrophilic peptide.

Sequence comparison of selected peptides

The sequence similarity of all studied peptides and indexed peptides were analyzed and compared using https://www.ebi.ac.uk/Tools/msa/clustalo. This tool allows for the alignment and comparison of peptide sequences, enabling researchers to identify conserved regions and motifs that may be important for the function or structure of the peptides. The information obtained from sequence comparison can be used to optimize and design peptide-based therapies for various diseases, including infections, cancer, and autoimmune disorders. Furthermore, sequence comparison can provide insights into the evolutionary relationships between peptides and their origins, which can aid in understanding their biological functions and potential applications.

The initial design of the new chimeric peptide based on the secondary structure

Comparison of the secondary structure of selected peptides

The secondary structure of all selected peptides was predicted online using GOR IV, which can be accessed at http://abs.cit.nih.gov/gor. The residues of the peptides involved in forming the helix structure, beta sheets, coil, and extended strand were then predicted. Finally, the secondary structure of 5 indexed peptides was compared to determine if there were any commonalities among them. In other words, all peptides were initially compared in terms of their secondary structures and five peptides selected as efficient indicators were further compared to each other in terms of their secondary structures. This comparison was conducted to identify common structural features among the efficient peptides against *A. baumannii* and to aid the integration of peptide sequences for designing more effective peptides.

Sequence integration of studied peptides based on the secondary structure

The scores of all peptides were predicted using the online software AntiBP2. Based on the literature, the peptides were divided into 2 categories: 1. peptides that affected *A. baumannii* and 2. functional peptides that have demonstrated superior performance *in vivo* and *in vitro* compared to other effective peptides. Peptides possessing a high spectrum of effectiveness, low toxicity for eukaryotic cells, low effective concentration, and short duration of action were considered functioning peptides. They were more effective than other peptides against *A. baumannii.*

To integrate the groups of peptides based on their secondary structure, we focused on the amino acid sequences that formed the helical regions, which are typically found in the middle of the peptide, as considered in Part C. Part A was defined as the section of peptide from the beginning of the peptide to the beginning of Part C (the N-terminal end), while Part B was defined as the section of the peptide from the end of Part C to the end of the peptide (the C-terminal end). In Sections A and B, several amino acids exhibited secondary structures such as coil or extended. Several amino acids at both ends of the peptide in Sections A and B were left unchanged to create a fusion of subunits. If any amino acids in Sections A and B formed a different structure, the amino acid sequence between them and Section C was removed. This approach was used to generate alternative fusion configurations (Fig. S1).

Optimization of the number of amino acids of the new chimeric peptides designed based on the secondary structure

The combined sequences of peptides with the highest score were selected. To calculate the average amino acid length of AMPs, all peptides in the AntiBP2 database were analyzed for their number of amino acids. The number of amino acids in the combined peptides was then optimized to maximize the score increase. Then, the combined peptides were compared according to their

physicochemical properties, their secondary structure (including helical wheels), the distribution of hydrophobic/hydrophilic amino acids (using the HeliQuest site at https://heliquest.ipmc.cnrs.fr), and the third structure using online software iterative threading assembly refinement (I-TASSER). Finally, those with the best results were selected as the new chimeric peptides for further analysis.

Designing based on the third structure of Musca domestica cecropin and pexiganan peptides

M-PEX1, a newly designed peptide, was selected for further analyses due to its partially helical third structure. M-PEX1 was created by combining some epitopes of *Musca domestica* cecropin (MDC) and pexiganan peptides. The tertiary structure of the parental peptides was examined using the I-TASSER online tool at https://zhanggroup.org/I-TASSER. Then, the amino acid sequences involved in creating the helix structure were identified using Accelrys DS visualizer software, and a new peptide was designed by combining them. The score of this newly designed peptide was calculated.

Designing the new chimeric peptide based on the similarity of the amino acid sequence of MDC and pexiganan peptides

Primary design and optimization

The type and order of amino acids in MDC and pexiganan peptides were compared in this method. The epitopes with the highest similarity from each parental peptide were used as the basis for designing new peptides. The one with the highest score was selected as the initial sequence among all sequences resulting from combining the fragments. The initial sequence was then analyzed for its tertiary and optimized by decreasing the number of amino acids to improve the score. Additionally, the presence of helix structures in the second and third structures was compared.

Amino acid modification to increase the helix structure

The peptide sequence was optimized by altering some amino acids to have the highest helix structure and lowest number of amino acids with the least impact on the score.

Identification of the secondary structure of the newly designed chimeric peptides by circular dichroism

Circular dichroism (CD) spectroscopy is an essential tool for determining the structure of proteins and peptides in membranes. Two new chimeric peptides called M-CIT (amino acid sequence: GWLKKGGKKIIQTAANVAGLF DVIL) and M-PEX12 (amino acid sequence: GWLKFKKKVAILTDIIQAVALG) were synthesized by GENSCRIP in China. CD spectroscopy (with five scans per sequence) was performed to identify their secondary structure. The mean residual ellipses of peptides were determined by CD spectroscopy using the Jasco J-810 spectroscopy device (Jasco, Japan) at room temperature and a scanning speed of 100 nm/min. For this purpose, 0.0018 mol/L of peptide water was loaded into a 0.5 cm quartz cell, and its spectrum was scanned from 180 to 240 nm (15).

Molecular dynamics simulation

Molecular simulation was used to predict and analyze the structural properties of the specifically designed chimeric peptides (M-PEX and M-CIT) to confirm the presence of helix structures. The initial 3D structures of the peptides were predicted by the I-TTASER online server. A mixture of palmitoyl-oleoyl-phosphatidylglycerol and palmitoyl-oleoyl-phosphatidylethanolamine lipids with a ratio of 3:1 for *A. baumanii* was used based on a previous study (21). The initial coordinates and topologies of the lipid bilayers were created using the CHARMM-GUI website (22). To provide well-equilibrated systems, all pure bilayers were simulated for 150 ns, and the last snapshots of the systems were used as the initial coordinates for each peptide bilayer simulation (23). Both peptides were amphipathic and placed in a parallel orientation to the surface of the model membranes (24). All molecular dynamics (MD) simulations were carried out using the GROMACS 5.1.2 package (25), with the CHARMM force field applied to the peptides and all model membranes. The appropriate numbers of sodium and chloride ions were added to each simulation box to neutralize the systems. Periodic boundary conditions were used along all simulation box

axes in all simulation systems, and the transferable intermolecular potential 3-point water model was applied to solvate the systems. The LINCS algorithm was used to constrain all covalent bonds (26). Simulations were conducted using a 1.2-nm distance cutoff for the van der Waals interactions and short-range electrostatic interactions (27). The particle mesh Ewald algorithm was used to calculate long-range electrostatic interactions. All systems were energy-minimized using the steepest descent algorithm and then equilibrated using the constant number of particles, volume, and temperature (NVT) ensemble for 300 ps (28). Each system was gradually equilibrated using the constant number of particles, pressure, and temperature (NPT) ensemble, with the temperature maintained at 323 K using the Nose-Hoover algorithm temperature (29,30). During the NPT equilibration, the pressure was maintained at 1 bar by the Parrinello-Rahman barostat. Three independent MD simulations were performed in the current study based on a previous experimental study that identified lysine and threonine as crucial residues for antimicrobial activity (31).To determine the role of the residues in the activities of M-PEX12 and M-CIT, we calculated the radial distribution functions between lysine and threonine residues and the phosphorus atoms of the model membranes. Additionally, to evaluate the effects of the peptide on the cohesion and structure of lipid bilayers, we calculated the density distributions of atoms across the normal direction of the bilayer (32).

Measurement of minimum inhibitory concentration and minimum bactericidal concentration of newly designed chimeric peptides

The antimicrobial activity of the new chimeric peptides was determined using the minimum inhibitory concentration (MIC) method designed against the target bacterium, following the instructions of the Clinical and Laboratory Standards Institute. Briefly, *A. baumannii* was cultured for 24 h at 37 °C in a Müller-Hinton broth culture medium. The cultured bacterium was diluted to 0.5 McFarland turbidity, and then further diluted 50 times. A 100 µL volume of the dilution was poured into the microplates, and 100 µL of diluted bacteria were added to reduce bacterial concentration to 10^5 × 5 CFU/mL per well. The plates were incubated at 37 °C for 16 h. The highest dilution of the peptide with no growth and clear medium was considered the MIC of the peptide. To determine the minimum bactericidal concentration (MBC) of peptides, the clear wells showing no growth were incubated for an additional 24 h on solid Mueller-Hinton agar culture media. The lowest concentration of peptide that showed no growth was considered the MBC concentration (33). The antibiotic meropenem served as a positive control by inhibiting bacterial growth in all tests because most strains of *A. baumannii*, including the standard strain (*A. baumanii* ATCC19606) selected for conducting the experiments in the current study, are susceptible to this antibiotic (34).

Hemolytic activity of newly designed chimeric peptides

Ten mL of blood and 2.5 mL of the isotonic solution (0.9% saline or phosphate-buffered saline (PBS)) were mixed in a container and centrifuged at 1500 rpm for 10 min. The supernatant was then gently discarded, and the isolated red blood cells (RBC) were washed and prepared as 10% suspension. Different concentrations of the peptide solutions were prepared and split in 1.5 mL microtube (1.5 mL/well). Next, 10 µL of 10% RBC suspension was added to each tube containing peptide, and the mixture was gently shaken to ensure thorough mixing. A tube containing 0.5 mL of 0.9% saline and 100 µL of RBC suspension was considered the negative control, while another tube containing 0.5 mL of 0.9% saline, 25 µL of 1% Triton X-100 lubricant, and 100 µL of erythrocyte suspension was considered the positive control. The tubes were then incubated at 37 °C for 15 min. After incubation, the sample volume was doubled with 0.9% saline (1200 µL) and centrifuged at 1500 rpm for 5 min. Finally, the light absorption of the samples was measured at the wavelength of 540 nm, and the hemolysis percentage values were calculated using the following equation:

$$Percentage\ of\ hemolysis = \frac{Optical\ removal\ of\ peptide\ -\ containing\ samples\ -\ negative\ control\ optical\ absorption}{Positive\ control\ optical\ absorption\ -\ negative\ control\ optical\ absorption} \times 100$$

RESULTS

Selection of active peptides against A. baumannii

By a comprehensive literature review, 30 peptides with inhibitory effect on *A.baumannii* were extracted and examined for eight main physicochemical properties, including peptide length, net charge, pI, aliphatic, instability, Boman, and hydrophobicity indexes, as well as GRAVY (1). The threshold used for the characteristics was determined as illustrated in Table 1. Accordingly, 5 peptides were selected as indicators for their high effect spectrum, low toxicity for eukaryotic cells, low effective concentration, and short effective time (Table 2).

Comparison of the sequences of selected peptides

Using bioinformatics, the sequences of 31 peptides affecting *A. baumannii* were compared to find the epitopes among the 31 peptide sequences with similarities in the amino acid type (Fig. 1A). Sequences of 5 indicator peptides were also compared separately for the same parameter (Fig. 1B).

The primary design of a new chimeric peptide based on the secondary structure

Comparison of the secondary structure of selected peptides

Considering the important role of the peptide secondary structure in its function, the secondary structure of all selected peptides was examined. The results predicted about 80% helical and coil structure of the first and last amino acids in all peptides. In the next step, the score of all peptides comprising above 15 amino acids with no branch was obtained. As a result, 16 peptides with scores above 0.8 were identified and used for the next step.

Merging the sequences of the studied peptides based on the secondary structure

The sequence of the indexed peptides was combined with peptides with a score above 0.8 (Table 3). Repeats were strictly avoided in 2 fusion peptides, and they were completely separated from 2 families. For each combination, a maximum of 16 non-repetitive binding states of different peptide fragments were considered. The score of 360 sequences was calculated using the AntiBP2 site, among which 66 sequences had scores higher than the parental peptides. Additionally, 4 of these identified sequences had a score above 2. For the fusion, the sequences of peptides were divided into three main Parts A, B, and C. The first peptide sequence with a score > 2 was the GGLRSLGRKILRAWKKYGPVAVVGQAT QIAKK with a score of 2.018 and 32 amino acids, which was a combination of 2 peptides of cecropin A and BMAP-28. The first 19 resides (GGLRSLGRKILRAWKKYGP) from BMAP-28 peptide included Parts A and C, and the remaining residues (VAVVGQATQIAKK) from cecropin A included Part B. The other parts of the two parental peptides were removed, as shown in Fig. 2. The second peptide sequence with a score > 2 was GWLKKIGKKIERVATIQTIGVAQQAANV AKKVASVIGGL with a score of 2.129 and 39 amino acids combined from MDC and citropin 1.1 peptides. The first 30 residues (GWLKKIGKKIERVVATIQTIGVAQQAAN VA) from Part MDC included Parts A and C, and the remaining part (KKVASVIGGL) derived from citropin 1.1 included Part B. The third peptide sequence with a score > 2 was GWLKKIGKKIERVGQHTRDATIQTIGVA QQAANVAGKAFVKILKK with a score of 2.108 and had 45 amino acids combined from MDC and pexiganan peptides. The first 35 residues derived from MDC (GWLKKIGK KIERVG QHTRDATIQTIGVA QQAANVA) included Parts A and C. The remaining sequence (GKAFVKILKK) taken from pexiganan included Part B. The fourth and last peptide with a score > 2 was a different combination of MDC and pexiganan, which included a 39-amino acid sequence of GWLKKIGK KIERVATIQTIGVAQQAANV AGKAFVKILKK with a score of 2.097. In this peptide, the first 29 residues (GWLKKIGKKIERVATIQ-TIGVAQQAA NVA) from MDC included Parts A and C, and the remaining sequence (GKAFVKILKK) from pexiganan included Part B (Table 4).

Table 1. List of peptides examined against *Acinetobacter baumannii*.

Peptide name	Amino acid sequencer (No.)	pI	Boman index (kcal/mol)	Molecular mass (Da)	Aliphatic index	Charge	Hydrophobicity	GRAVY	Instability index
P307	NAKDYKGAAAEFPKWNKAGGRVLAGLVKRRK (amino acids 108 to 138) (31)	10.70	2.23	3400.98	63.23	+7	38%	-0.861	54.08
P307AE-8	NAKDYKGAAAEFPKWNKAGGRVLAGLVKRRKAEMELFLK (original) (39)	10.21	1.82	4363.15	72.82	+6	43%	-0.603	42.86
P307SQ-8C	NAKDYKGAAAEFPKWNKAGGRVLAGLVKRRKSQSRESQC (from hepatitis B virus) (39)	10.38	2.84	4306.92	50.26	+7	33%	-1.067	74.12
P307CS-8	NAKDYKGAAAEFPKWNKAGGRVLAGLVKRRKCSQRQSES (scramble) (39)	10.38	2.84	4306.92	50.26	+7	33%	-1.067	76.06
P307SQ-8A	NAKDYKGAAAEFPKWNKAGGRVLAGLVKRRKSQSRESQA (39)	10.69	2.82	4274.86	52.82	+7	33%	-1.085	76.06
BMAP-28	GGLRSLGRKILRAWKKYGPIIVPIIRI (27)	12.02	0.87	3074.84	144.44	+7	44%	0.256	49.57
A837	GGLRKLGRKILRAWKKYGPIIVPIIRI (27)	12.02	0.95	3115.94	144.44	+8	44%	0.141	30.16
A838	KGLRKLGRKILRAWKKYGPI IVPIIRI (27)	12.02	1.19	3187.06	144.44	+9	44%	0.011	22.44
A839	GGLRSLGRKILRAWKKGGPIIVPIIRI (27)	12.48	0.83	2968.72	144.44	+7	44%	0.289	54.14
A840	KGLRKLGRKILRAWKKGGPIIVPIIRI (27)	12.49	1.15	3080.94	144.44	+9	44%	0.044	27.01
TP3	FIHHIIGGLFSVGKHIHSLIHGH (23)	8.79	-0.34	2557.00	131.30	+7	43%	0.591	57.34
TP4	FIHHIIGGLFSAGKAIHRLIRRRRR (25)	12.70	2.62	2981.60	117.20	+7	44%	-0.128	130.24
cod Pis 1	FIHHIIGWISHGVRAIHRAIHG (22)	12.00	0.51	2527.97	128.64	+7	50%	0.441	42.53
Magainin 2	GIGKFLHSAKKFGKAFVGEIMNS (23)	10.00	0.41	2466.93	72.17	+3	43%	0.083	-0.10
Cathelicidin BF-30	KFFRKLKKSVKKRAKEFFKKPRVIGVSIPF (30)	11.79	2.12	3638.54	71.33	11	40%	-0.537	9.34
Apo5 APOC164-88	FSTKTRNWFSEHFKKVKEKLKDTFA (25)	10.00	2.85	3103.57	31.20	+4	32%	-1.148	-7.50
Apo6 APOC167-88	KTRNWFSEHFKKVKEKLKDTFA (22)	10.00	3.1	2768.21	35.45	+4	31%	-1.364	-9.89
A1P394-428	PPPVIKFNRPFLMWIVERDTRSILFMGKIVNPKAP (35)	11.00	1.02	4109.01	94.57	+4	45%	0.017	94.57
LL-37	LLGDFFRKSKEKIGKEFKRIVQRIKDFLRNLVPRTES (37)	10.61	2.99	4493.32	89.46	+6	35%	-0.724	23.34
MDC	GWLKKIGKKIERVGQHTRDATIQTIGVAQQAANVAATLKG (40)	10.56	1.43	4257.95	95.25	+5	40%	-0.323	14.98

Table 1. Continued

Peptide name	Amino acid sequencer (No.)	pI	Boman index (kcal/mol)	Molecular mass (Da)	Aliphatic index	Charge	Hydrophobicity	GRAVY	Instability index
Aurein 1.2	GLFDIIKKIAESF (13)	6.07	0.12	1480.77	127.69	+1	53%	0.669	20.48
CAMEL (CM15)	KWKLFKKIGAVLKVL (15)	10.60	-0.53	1771.31	149.33	+5	60%	0.540	-28.99
Citropin 1.1	GLFDVIKKVASVIGGL (16)	8.59	-1.01	1615.98	158.12	+2	56%	1.281	14.19
Omiganan	ILRWPWWPWRRK (12)	12.30	2.59	1780.16	65.00	+4	50%	-1.325	131.93
r-Omiganan	KRRWPWWPWRLI (12)	12.30	2.59	1780.16	65.00	+ 4	50%	-1.325	127.00
Pexiganan	GIGKFLKKAKKFGKAFVKILKK (22)	10.90	0.49	2478.20	93.18	+ 9	45%	-0.159	-6.16
CM11	WKLFKKILKVL (11)	10.48	-0.62	1415.858	168.18	+ 4	63%	0.581	-17.94
Cecropin A	KWKLFKKIEKVGQNIRDGIIKAGPAVAVVGQATQIAKK (38)	10.47	0.97	4133.00	105.26	+7	44%	-0.174	16.35
Melittin	GIGAVLKVLTTGLPALISSWIKRKRQQ (27)	12.02	0.67	2934.559	130.00	+5	44%	0.2333	50.58

MDC, *Musca domestica* cecropin.

Table 2. Selected peptides as indicators along with physicochemical properties.

Peptide name	Amino acid sequencer	pI	Boman index (kcal/mol)	Molecular mass (Da)	Aliphatic index	Charge	Hydrophobicity	GRAVY	Instability index
P307SQ-8C	NAKDYKGAAAEFPKWNKAGGRVLAGLVKRRKSQSRESQC (from hepatitis B virus) (39)	10.38	2.84	4306.92	50.26	+7	33%	-1.067	74.12
BMAP-28	GGLRSLGRKILRAWKKYGPIIVPIIRI (27)	12.02	0.87	3074.84	144.44	+7	44%	0.256	49.57
TP4	FIHHIIGGLFSAGKAIHRLIRRRRR (25)	12.70	2.62	2981.60	117.20	+7	44%	-0.128	130.24
Magainin 2	GIGKFLHSAKKFGKAFVGEIMNS (23)	10.00	0.41	2466.93	72.17	+3	43%	0.083	-0.10
MDC	GWLKKIGKKIERVGQHTRDATIQTIGVAQQAANVAATLKG (40)	10.56	1.43	4257.95	95.25	+5	40%	-0.323	14.98

MDC, *Musca domestica* cecropin.

Fig. 1. Sequence comparison of peptides affecting *A. baumannii*. (A) All retrieved peptides and (B) specific peptides with high efficiency. MDC, *Musca domestica* cecropin.

Table 3. Combination of indicator peptides with high-score peptides. Similar items shown in Bold were removed during the design.

Indicator peptides				
P307SQ-8C	**BMAP-28**	**TP4**	**Magainin 2**	**MDC**
P307-P307SQ-8C	P307-BMAP-28	P307-TP4	P307-magainin 2	P307-MDC
BMAP-28 P307SQ-8C	**BMAP-28-BMAP-28**	BMAP-28-TP4	BMAP-28-magainin 2	BMAP-28-MDC
A837-P307SQ-8C	A837-BMAP-28	A837-TP4	A837-magainin 2	A837-MDC
A838-P307SQ-8C	A838-BMAP-28	A838-TP4	A838-magainin 2	A838-MDC
A839-P307SQ-8C	A839-BMAP-28	A839-TP4	A839-magainin 2	A839-MDC
A840-P307SQ-8C	A840-BMAP-28	A840-TP4	A840-magainin 2	A840-MDC
TP4-P307SQ-8C	**TP4-BMAP-28**	**TP4-TP4**	TP4-magainin 2	TP4-MDC
Magainin 2-P307SQ-8C	**Magainin 2-BMAP28**	**Magainin 2-TP4**	**Magainin 2-magainin 2**	Magainin 2-MDC
CBF30-P307SQ-8C	CBF30-BMAP-28	CBF30-TP4	CBF30-magainin 2	CBF30-MDC
LL-37-P307SQ-8C	37-LL-BMAP-28	LL-37-TP4	LL-37-magainin 2	LL-37-MDC
MDC-P307SQ-8C	**MDC-BMAP-28**	**MDC-TP4**	**MDC-magainin 2**	**MDC-MDC**
CM15-P307SQ-8C	CM15-BMAP-28	CM15-TP4	CM15-magainin 2	CM15-MDC
Citropin 1.1-P307SQ-8C	Citropin 1.1-BMAP-28	Citropin 1.1-TP4	Citropin 1.1-magainin 2	Citropin 1.1-MDC
Pexiganan-P307SQ-8C	Pexiganan-BMAP-28	Pexiganan-TP4	Pexiganan-magainin 2	Pexiganan-MDC
Cecropin A-P307SQ-8C	Cecropin A-BMAP-28	Cecropin A-TP4	Cecropin A-magainin 2	Cecropin A-MDC

MDC, *Musca domestica* cecropin.

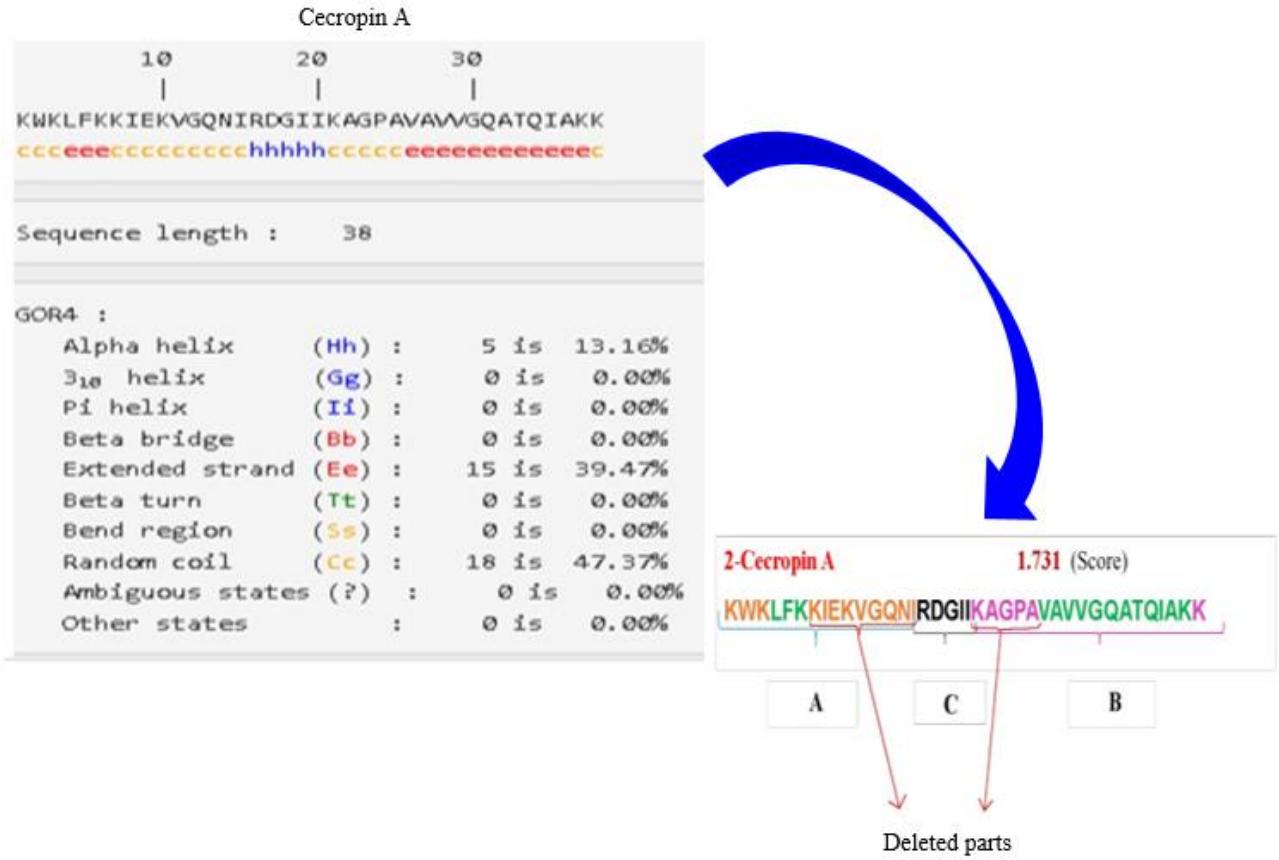

Fig .2. Deletion of sequences with identical secondary structures on both sides of Fragment C.

Table 4. Sequence of parental peptides with their scores and different models of combination. Combination models included (a) the method of combining 2 peptides cecropin A and BMAP-28, (b) the method of combining 2 peptides citropin1.1 and MDC, (c) the method of combining 2 peptides pexiganan and MDC. Rows highlighted by gray color, sequences with a score above 2; the black part of the sequence is, the amino acid sequence forming the helix structure; the orange part of the sequence, amino acid sequence forming the coil structure; green part of the sequence, the sequence of amino acids that made up the extended structure; 112, parts A and C of peptide number 1 and part B of peptide number 2, respectively (from left to right); 221, parts A and C from peptide number 2 and part B from peptide number 1, respectively (left to the right). Score of peptides with less than 15 sequences were not identified by ANTIBP2 and are denoted by "?". Parental peptides were considered to have antimicrobial properties, so the score section has been left blank.

	Name	Sequence	Score ANTIBP2
1	BMAP-228	GGLRSLGRKILRAWKKYGPIIVPIIRI	-
2	Cecropin	KWKLFKKIEKVGQNIRDGIIKAGPAVAVVGQATQIAKK	-
3	112	GGLRSLGRKILRAWKKYGPKAGPAVAVVGQATQIAKK	1.774
4	122	GGLRSLGRDGIIKAGPAVAVVGQATQIAKK	0.910
5	211	KWKLFKKIEKVGQNIRKILRAWKKYGPIIVPIIRI	0.787
6	221	KWKLFKKIEKVGQNIRDGIIIIVPIIRI	0.515
7	112.2	GGLRSLGRKILRAWKKYGPVAVVGQATQIAKK	2.018
8	122.2	GGLRSLGRDGIIVAVVGQATQIAKK	0.481
9	2.211	KWKLFKRKILRAWKKYGPIIVPIIRI	0.613
10	2.221	KWKLFKRDGIIKAGPAVAVVGQATQIAKK	1.729
11	MDC	GWLKKIGKKIERVGQHTRDATIQTIGVAQQAANVAATLKG	-
12	Citropin 1.1	GLFDVIKKVASVIGGL	-
13	112	GWLKKIGKKIERVGQHTRDATIQTIGVAQQAANVAKKVASVIGGL	1.726
14	122	GWLKKIGKKIERVGQHTRDKKVASVIGGL	1.134
15	211	GLFDVIATIQTIGVAQQAANVAATLKG	0.572
16	221	GLFDVIATLKG	?
17	1.112	GWLKKIGKKIERVATIQTIGVAQQAANVAKKVASVIGGL	2.129
18	1.122	GWLKKIGKKIERVKKVASVIGGL	1.018

Table 4. Continued

	Name	Sequence	Score ANTIBP2
19	MDC	GWLKKIGKKIERVGQHTRDATIQTIGVAQQAANVAATLKG	-
20	Pexiganan	GIGKFLKKAKKFGKAFVKILKK	-
21	112	GWLKKIGKKIERVGQHTRDATIQTIGVAQQAANVAGKAFVKILKK	2.108
22	122	GWLKKIGKKIERVGQHTRDKAKKFGKAFVKILKK	1.232
23	211	GIGKFLKATIQTIGVAQQAANVAATLKG	1.325
24	221	GIGKFLKKAKKFATLKG	0.859
25	112.2	GWLKKIGKKIERVGQHTRDATIQTIGVAQQAANVAKAFVKILKK	1.951
26	122.2	GWLKKIGKKIERVGQHTRDKAKKFKAFVKILKK	1.178
27	1.112	GWLKKIGKKIERVATIQTIGVAQQAANVAGKAFVKILKK	2.097
28	1.112.2	GWLKKIGKKIERVATIQTIGVAQQAANVAKAFVKILKK	1.861
29	1.122	GWLKKIGKKIERVKAKKFGKAFVKILKK	0.878
30	1.122.2	GWLKKIGKKIERVKAKKFKAFVKILKK	0.790
31	2.211	GIGKATIQTIGVAQQAANVAATLKG	0.803
32	2.221	GIGKKAKKFATLKGG	0.301

MDC, *Musca domestica* cecropin.

Optimizing the number of amino acids of new chimeric peptides based on the secondary structure

Analysis of the AntiBP2 database demonstrated that most AMPs had a length of 20 to 25 amino acids (Fig. S2). Accordingly, we tried optimizing the combined peptides by eliminating some amino acids to increase their score. The following peptides were four optimal sequences including:

1. the M-CIT chimeric peptide containing 24 residues with the sequence of GWLKKGKKIIQTAANV AGLFDVIL, with a score of 995, hydrophobicity of 54%, a total charge of +3, GRAVY of 0.525, and Boman index equal to -0.22 kcal/mol; 2. the B-CEC peptide containing 21 residues with the optimal sequence of GGLSLKILWKGA VVQATIAKK, with a score of 2.823, hydrophobicity of 52%, a total charge of +4, GRAVY of 0.547, and Boman index of -0.45 kcal/mol; 3. the M-PEX1 peptide containing 22 residues with the optimal sequence of GWLKKIVGITIGVQAN AAFLKK, with a score of 2.823, hydrophobicity of 54%, a total charge of +4, GRAVY of 0.559, and Boman index of 0.42 kcal/mol; and 4. M-PEX2 chimeric peptide comprised 20 residues with the optimal sequence of GLKGKKIRIT IGVQNAAFVL, a score of 2.843, hydrophobicity of 50%, a total charge of +4, GRAVY of 0.540, and Boman index equal to 0.21 kcal/mol (Fig. S3).

Results of structural analysis of optimized peptides designed based on the secondary structure

The physicochemical and structural properties of optimized peptides were obtained and compared with those of the parental ones. M-CIT was the only acceptable optimized peptide in terms of the tertiary structure, showing a helical structure similar to parental peptides. Therefore, 3 other peptides (B-CEC, M-PEX1, and M-PEX2) were no longer included in further analyses (Fig. 3). Then, the M-CIT new chimeric peptide was compared with those of MDC and citropin, and found to have the most similar amino acid sequence to the parental peptides, with a sufficient dispersion in the hydrophobic and hydrophilic amino acids (Fig. 4).

Peptide design based on the tertiary structure of 2 peptides, MDC and pexiganan

The M-PEX1 peptide was a combination of epitopes from 2 parental peptides, consisting of MDC with 2 helical structures and pexiganan with one helical structure, based on the I-TASSER site. The amino acid sequence of helical structures in 2 parental peptides was determined using the Accelrys DS visualizer software. The helix-forming sequences in the MDC peptide were WLKKIGKKIERV GQHTRD and TIQTIGVAQQAANVAAT. The helix-forming sequence in the pexiganan peptide was IGKFLKKAKKFGKKA. Sequences were designed based on the combination and rearrangement of the epitopes, none of which produced the desired score (Fig. 5).

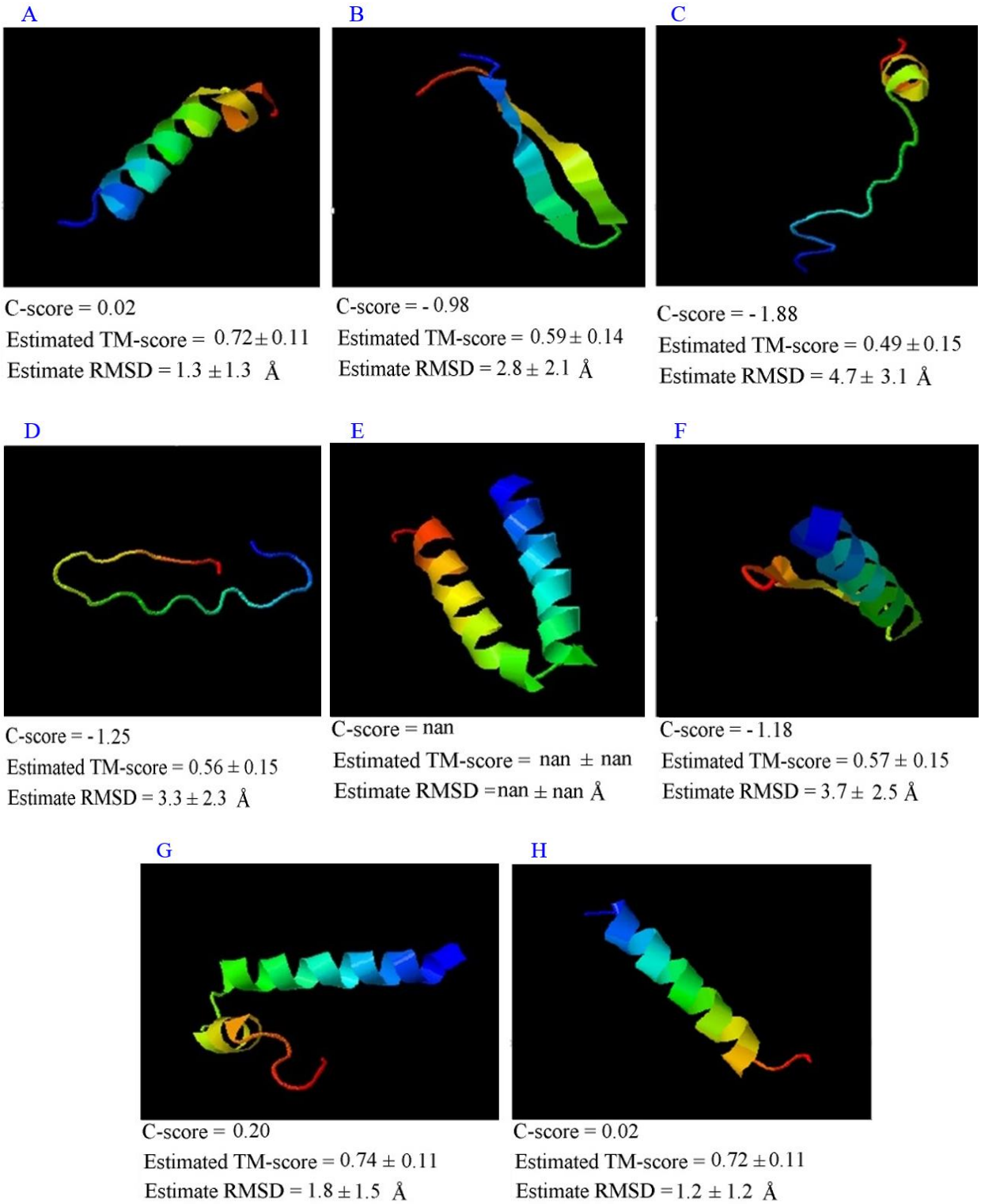

Fig .3. Three-D structure of new chimeric peptides based on the secondary structure. (A-D) Newly designed peptides and (E-H) parental peptides. Only Peptide A with M-CIT was predicted to have a helical structure similar to parental peptides. RMSD, Root mean square deviation; TM, a metric for assessing the topological similarity of protein structures.

A

```
CLUSTAL O(1.2.4) multiple sequence alignment


Citropin        GLFDVIKKVASVIGGL------------------------  16
(Mdc)           GWLKKIGKKIERVGQHTRDATIQTIGVAQQAANVAATLKG  40
M-CIT:          GWLKKGKKIIQTAANVAGLFDVIL----------------  24
                * :.   *  .  .
```

B

```
          10        20
           |        |
   GWLKKGKKIIQTAANVAGLFDVIL          Sequence length :    24
   ccccccchhhhhhhhhhceeceec

GOR4 :
   Alpha helix      (Hh) :    10 is  41.67%      Beta turn        (Tt) :     0 is   0.00%
   3(10) helix      (Gg) :     0 is   0.00%      Bend region      (Ss) :     0 is   0.00%
   Pi helix         (Ii) :     0 is   0.00%      Random coil      (Cc) :    10 is  41.67%
   Beta bridge      (Bb) :     0 is   0.00%      Ambiguous states (?)  :     0 is   0.00%
   Extended strand  (Ee) :     4 is  16.67%      Other states          :     0 is   0.00%
```

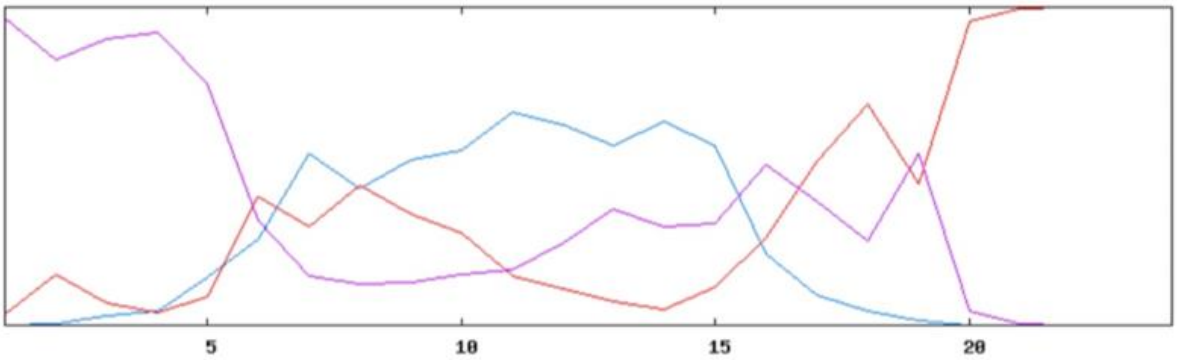

C

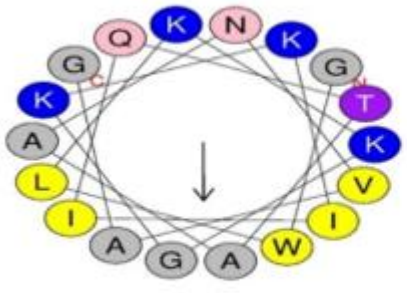

D

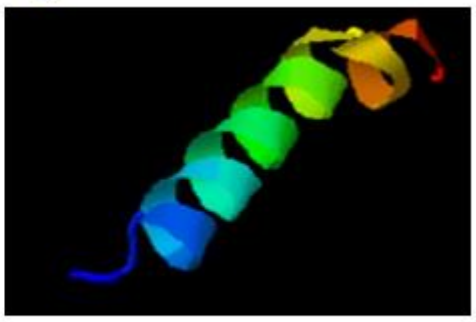

C-score = 0.02
Estimated TM-score = 0.72 ± 0.11
Estimated RMSD = 1.3 ± 1.3 Å

Fig .4. Analysis of optimized peptides designed based on the secondary structure. (A) Comparison of the new M-CIT chimeric peptide sequence with the parental sequence; (B) prediction of the secondary structure of the M-CIT peptide sequence by GOR IV software; (C) wheel cycle of the newly designed peptide M-CIT by HeliQuest; (D) the 3D structure of the M-CIT peptide. MDC, *Musca domestica* cecropin; RMSD, root mean square deviation; TM, a metric for assessing the topological similarity of protein structures.

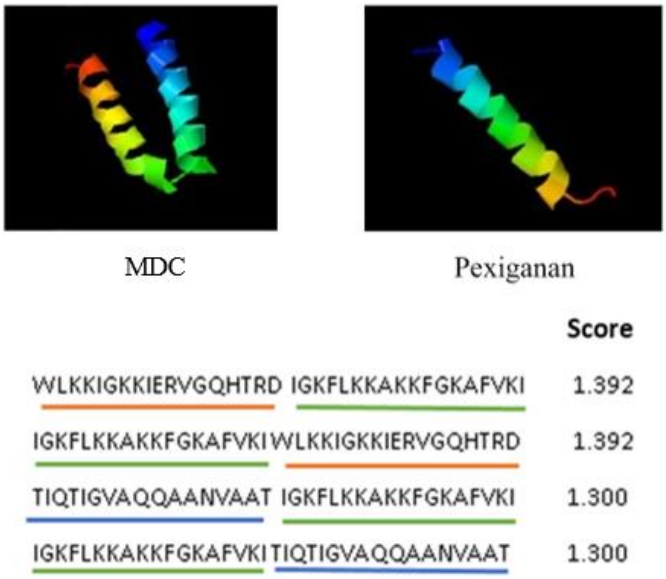

Fig. 5. The juxtaposition of sequences of peptides that form the helix structure and record their scores. Green sequence, helix structure sequence generator in pexiganan peptide; blue and orange sequences, the 2 constituents of the helix structure in the MDC peptide; MDC, *Musca domestica* cecropin.

Designing based on amino acid sequence similarity of 2 peptides MDC and pexiganan

Primary design and optimization

Based on the previous study (9), it was found that the GWLK sequences in the MDC peptide were in the optimal position and therefore, were kept intact. The sequence FLKKAKKFGK AFVKILK from the pexiganan peptide, which exhibited the highest similarity to the MDC peptide, was inserted after the GWLK sequence in the MDC peptide. The resulting initial sequence with a score of 1.987 was designed as follows: GWLKFLKKAKKFGKAFVKILK TRDATIQTIGVAQQAANVAATLKG. The 3D structure prediction for this peptide showed that it had a generally helical tertiary structure and was overall similar to the structure of the parental peptides (Fig. 6).

After removing certain amino acids from the initial sequence, the secondary structure and score were predicted and compared again, and the following sequences were identified as appropriate: 1. a 25-amino acid sequence (GWLKFKKKGAKILTDIIVQANVALG) with a score of 2.976; 2. a 24-amino acid sequence (GWLKFKKKGAGATTIIVQANV ALG) with a score of 2.995; and 3. a 23-amino acid sequence (GWLKFKKKGAILTDIIQ ANVALG) with a score of 2.995. The third sequence, which consisted of 23 amino acids was the shortest and selected for the subsequent design steps because it showed the highest score and a suitable helical structure similar to the parental peptides in 3D structure prediction (Fig. 7).

Amino acid modification to increase the helical structure

We identified the substantial role of arginine and valine at positions 4, 9, and 23 by exploring point deletion and substitution, in creating the helical structure. We also observed that valine had the greatest impact on the score of the resulting peptide. Therefore, in the main peptide, lysine (K) at position 4 and glycine at positions 9 and 23 were substituted with valine.

The highest score was obtained by substituting valine at position 9 and optimizing the number of amino acids, accordingly. As a result, the following optimal sequences were obtained for the new chimeric peptide, M-Pex12: GWLKFKKKVAILTDIIQAVALG, with 22 residues. This new chimeric peptide had a hydrophobicity of 59%, a total charge of +3, a GRAVY score of 0.75, and a Boman index of -0.5 kcal/mol. In addition, it showed a helical structure in 3D prediction assays and was named M-Pex12 (Fig. 8).

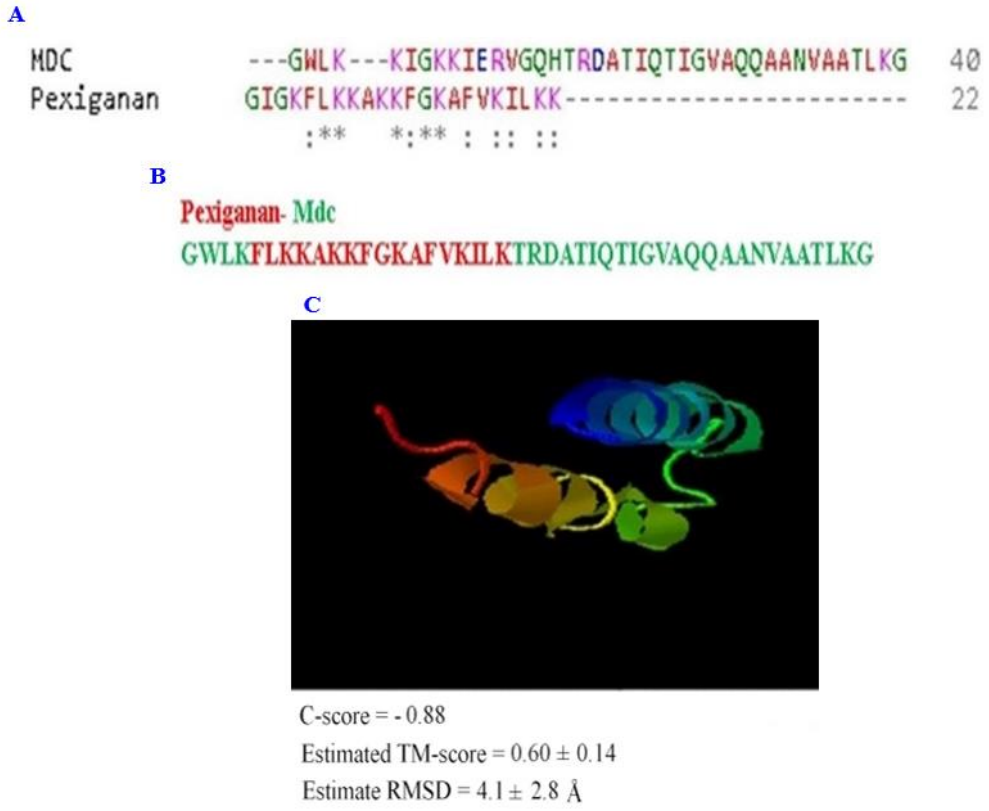

Fig .6. Designing based on amino acid sequence similarity of 2 peptides MDC and pexiganan. (A) Comparison of the sequence similarity of the 2 parental peptides MDC and pexiganan; (B) the fusion sequence of the 2 parental peptides (green, MDC peptides and the red, pexiganan); (C) the 3D structure of the primary M-Pex fusion peptide with 2 helix fragments that resemble the 3D structure of the parental peptide. MDC, *Musca domestica* cecropin; RMSD, root mean square deviation; TM, a metric for assessing the topological similarity of protein structures.

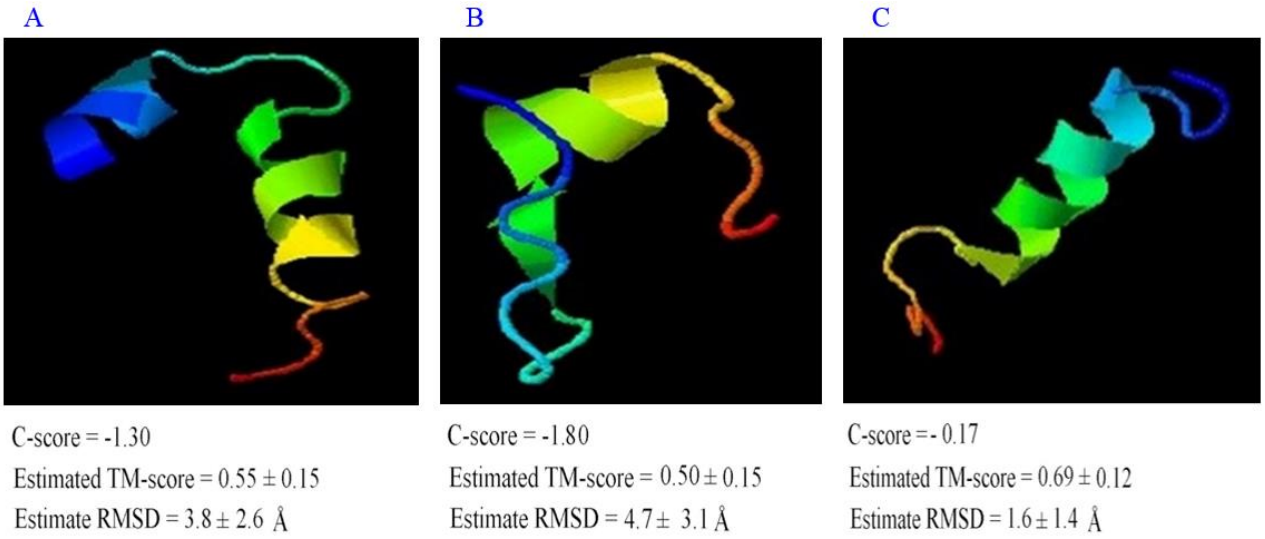

Fig .7. Three-D structure of the peptide sequence after selecting some amino acids in the M-Pex peptide design. (A) Three-D structure of 25-amino acid peptide M-Pex; (B) 3D structure of 24-amino acid M-Pex peptide; (C) 3D structure of 23-amino acid peptide M-Pex. RMSD, Root mean square deviation; TM, a metric for assessing the topological similarity of protein structures.

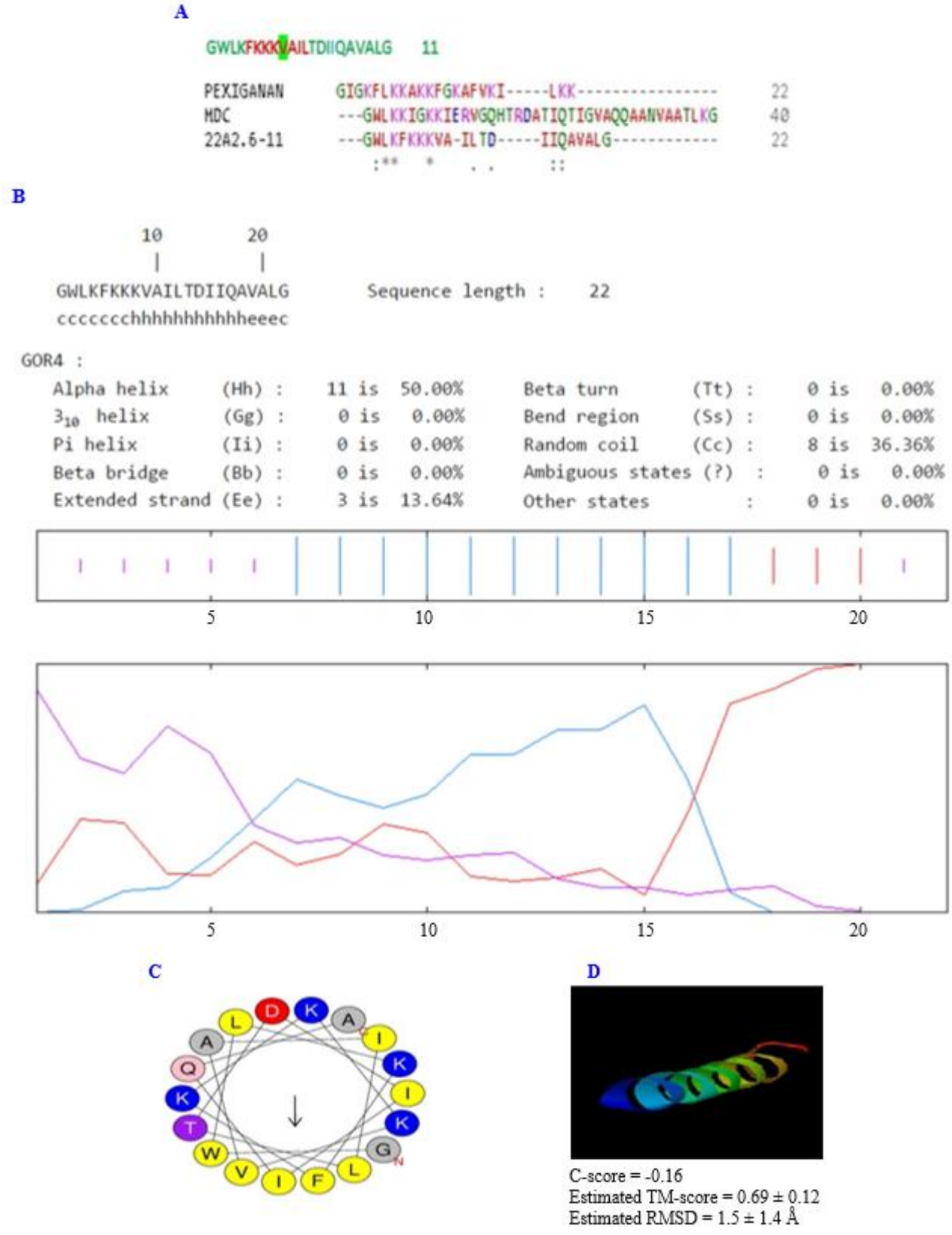

Fig .8. Analysis of optimized peptides designed based on amino acid modification. (A) Comparison of the sequence similarity of a new chimeric peptide called M-Pex12 (22 amino acids) with parental peptides; (B) the secondary structure of the second M-Pex12 peptide; (C) the wheel cycle of the M-Pex12 peptide; (D) the 3D structure of the M-Pex12 peptide. RMSD, Root mean square deviation; TM, a metric for assessing the topological similarity of protein structures.

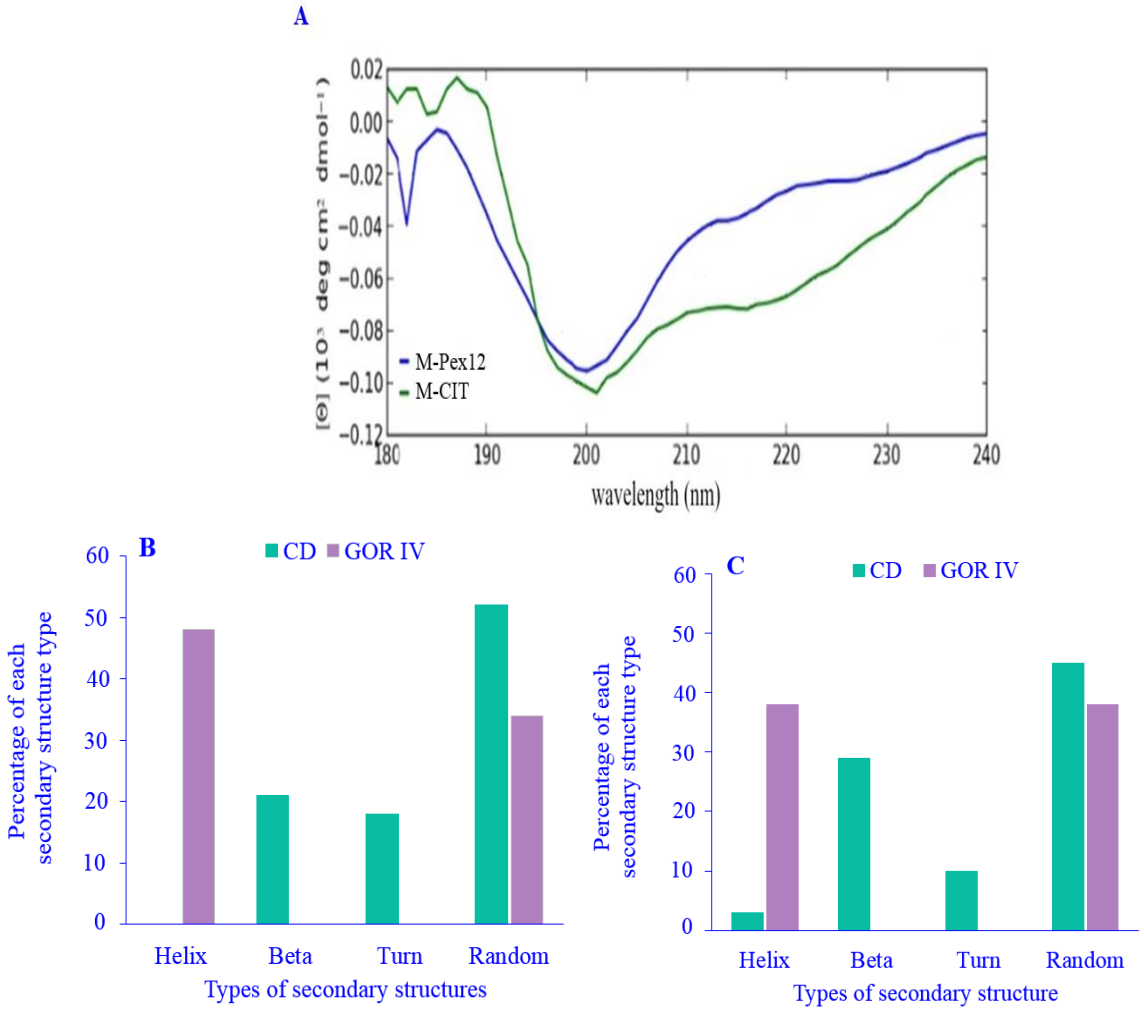

Fig .9. Identifying the secondary structure of the newly designed chimeric peptide by CD. (A) Recorded spectrum and CD analysis of 2 peptides M-Pex12 and M-CIT; (B) comparison of CD and bioinformatics analyses by GOR IV software for M-Pex12 peptide; (C) comparison of CD and bioinformatics analyses by GOR IV software for M-CIT peptide. CD, Circular dichroism.

Identifying the secondary structure of the newly designed chimeric peptide by CD

The M-CIT and M-Pex12 peptides were synthesized chemically with purities greater 95%. The results of CD analysis demonstrated that the M-PEX12 chimeric peptide had 0.0% helical structure, 25% beta structure, 20.30% turn structure, and 54.70% random structure in a water buffer. In contrast, the M-CIT chimeric peptide showed 5.3% helical structure, 36.80% beta structure, 13.30% turn structure, and 48.50% random structure in the same water buffer (Fig. 9).

Molecular dynamics simulation

According to MD analysis, it was observed that both M-CIT and M-PEX12 were capable of binding to the lipid bilayers of *A. baumanii*. To investigate the crucial role of certain residues in the functions of the newly designed peptides, the radial distribution was calculated between the side chains of lysine and threonine (T) and the phosphorus atoms of the model membranes. In both peptides, lysine indicated a peak at approximately 0.5 nm, while threonine showed a peak at around 1 nm. These results suggested that the side chains of these residues were positioned at an appropriate distance to enable hydrogen bonds and electrostatic interactions with the phosphorus atoms. The density profile of these peptides indicated that they overlapped with the head group regions, which suggested that these peptides were localized on the surface of the model membrane and evenly distributed. These findings collectively suggested that the newly designed peptides were likely to affect the outer membrane of bacteria (Figs. 10 and 11).

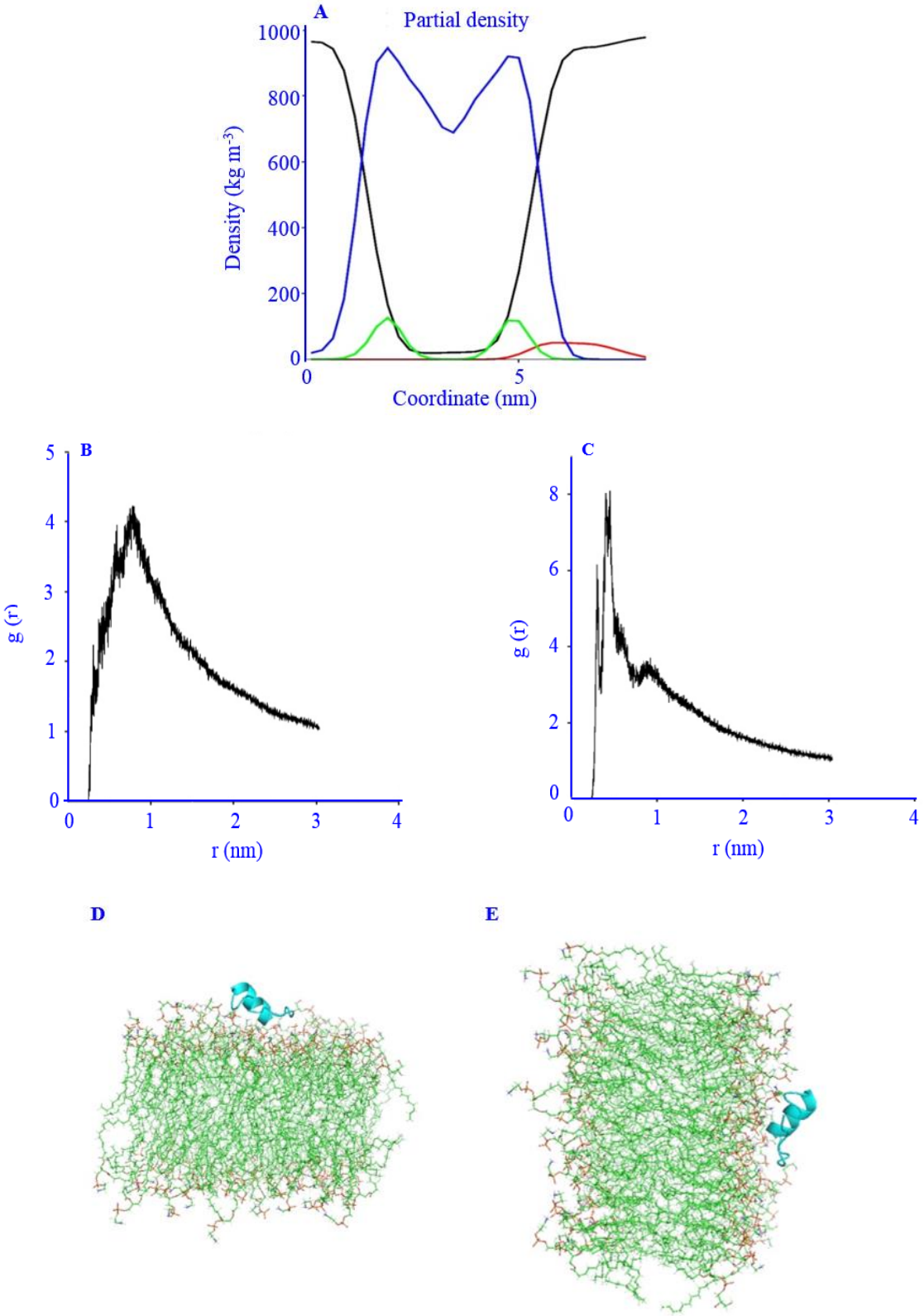

Fig .10. Prediction structure of M-Pex12. (A) Structure radial density; (B and C) RDF plots between the side chains of peptide in the references r-2 and r-4, respectively; initial orientation of peptide concerning the model membrane in (D) MD2 and (E) MD3 systems. The peptide and amino acid side chains were shown as cartoon and licorice models, respectively. The hydrophobic tail and phosphorus atom of lipid molecules were shown as line and sphere models, respectively. The RDF was denoted as g(r). This quantity represents the average distribution of atoms around any given atom within the system. The function of g(r) provides information about the probability of finding a particle at a distance "r" from a reference particle, relative to a randomly distributed set of particles. Blue color, peptide; green color, membrane; RDF, radial distribution function; MD, molecular dynamics.

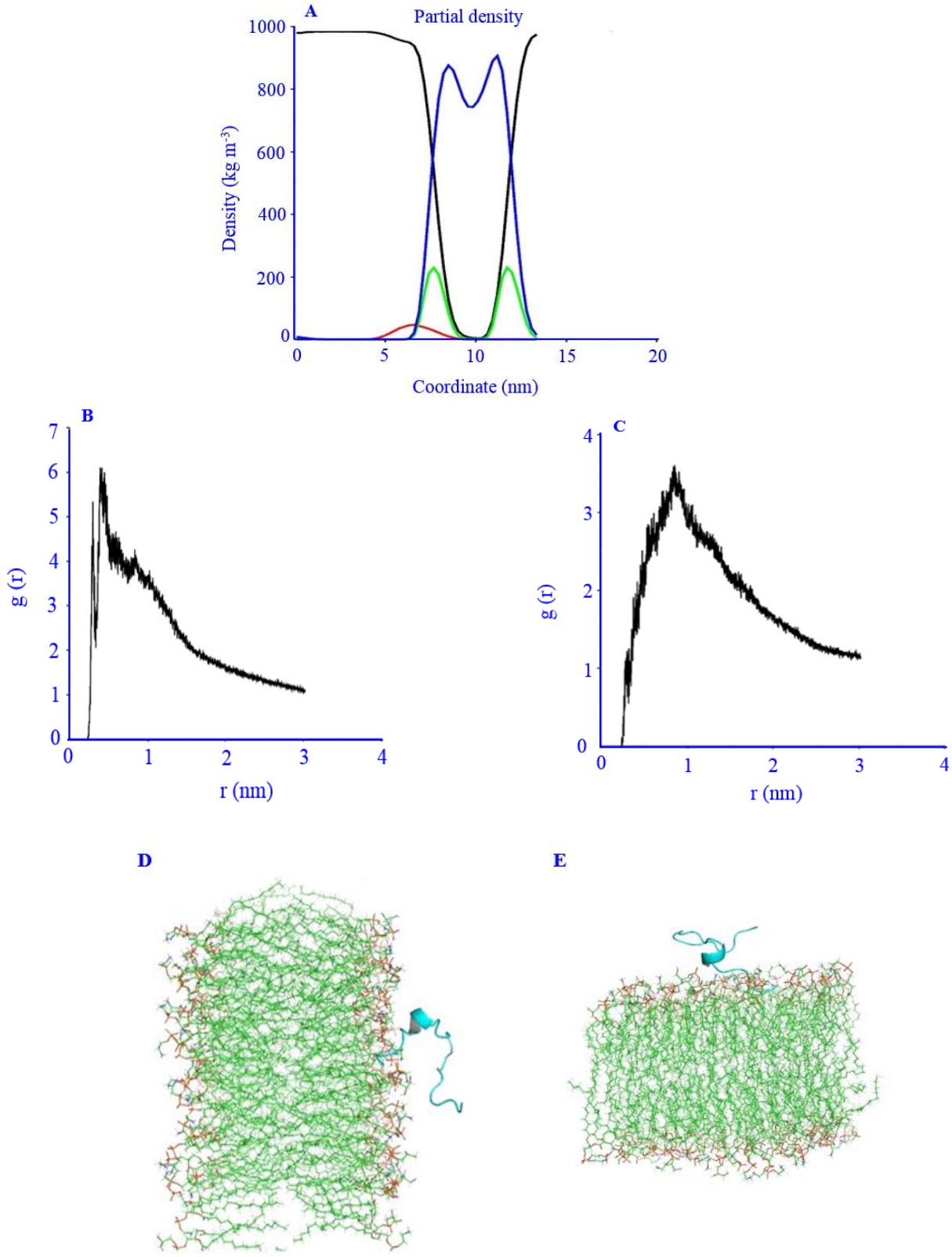

Fig .11. Prediction structure of M-CIT. (A) Structure radial density; (B and C) RDF plots between the side chains of peptide in the references r-4 and r-2, respectively; initial orientation of peptide concerning the model membrane in (D) MD2 and (E) MD3 systems. The RDF was denoted as g (r). This quantity represents the average distribution of atoms around any given atom within the system. The function of g (r) provides information about the probability of finding a particle at a distance "r" from a reference particle, relative to a randomly distributed set of particles. Blue color, peptide; green color, membrane; RDF, radial distribution function; MD, molecular dynamics.

Measurement of MIC in newly designed chimeric peptides

MIC and MBC tests were conducted on 2 newly designed chimeric peptides (M-CIT and M-PEX12) against the standard bacterial strain of *A. baumannii* ATCC 19606 using the broth microdilution method, with meropenem as the control antibiotic. The results indicated that only M-PEX12 showed antimicrobial activity against the target bacterial strain, with a MIC of 33.1 µM and MBC of 41.4 µM. In contrast, M-CIT displayed no significant activity against *A. baumannii* with an MIC of 187.5 µM and MBC of 375 µM.

Hemolytic activity of newly designed chimeric peptides

The toxicity of M-Pex12 and M-CIT peptides was evaluated using the RBC hemolysis test against human erythrocytes. In this test, a positive control containing Triton X100 and erythrocyte suspension was considered 100% hemolysis. Accordingly, M-PEX12 exhibited 0.72% hemolysis at the MIC concentration and 1% hemolysis at 2X MIC concentration, whereas M-CIT showed 1.24% hemolysis at a concentration of 41 µM and > 5% hemolysis at higher concentrations.

DISCUSSION

Bacterial resistance to multiple antibiotics is a major health concern, especially in the ICU, where infections can be difficult to treat. Additionally, ICU-acquired infections are responsible for causing 700,000 deaths worldwide annually (35,36).

Acinetobacter is a highly antibiotic-resistant pathogen, and there is a need to develop effective treatments against it. AMPs are being increasingly researched as a potential solution for this problem. Natural AMPs suffer limitations such as rapid degradation in the body and short half-life, as well as immunogenicity and toxicity against human cells. Physicochemical studies and bioinformatical manipulations in the sequence of natural peptides have helped experts to develop synthetic AMPs, which overcome the limitations and also expand their range of action (14). In the present study, novel chimeric peptides were developed through multiple methods based on the sequences of natural peptides discovered to be active against *A. baumannii*. For this purpose, the sequences of several peptides that were found to be active against the targeted bacterium were selected and used to design new peptides.

We observed that the ideal threshold for all characteristics of peptides affecting the target bacterium was not the same because, for example, the most effective peptide against *Acinetobacter* displayed less suitable physicochemical characteristics in comparison to those with lower antibacterial activity. Hence, we concluded that improving physicochemical properties was insufficient for designing a new chimeric peptide. We applied 3 different peptide designing methods using different online software. The first method involved using the online AntiBP2 software to compare the scores of different peptide sequences. This software predicts the peptide antimicrobial potency based on support vector machines, artificial neural networks, or quantitative matrices (37,38). AntiBP provided a general model based on 3 characteristics: 1. 15 N-terminal residues, 2. 15 C-terminal residues, and 3. a combination of 15 N- and 15 C-terminal residues using the APD3 database (9,37-39). Synthetic peptides were designed to be 22 - 25 residues because most AMPs have this length, according to the AMPs database 3 (APD3). Additionally, other peptides with functions other than antimicrobial properties are rarely found at this size. This study aimed to analyze the secondary structure of these peptides to identify common structures among peptides that affect *A. baumannii*. It was found that about 75% of the studied peptides had a helical structure. We also observed that both the N-terminal and C-terminal ends had a random coil structure in almost all peptides (except TP3). Accordingly, we attempted to synthesize a new peptide with 22 - 25 amino acids. The newly designed peptides were not significantly different from the parental peptides in terms of their secondary and tertiary structures and had a maximum helical structure. In the first peptide design method, which was based on the secondary structure, all desired peptides were examined and optimized for their secondary structure, length, and score. Then, fusion was performed without changing any amino acid to

obtain the highest score for the new peptide. As a result, 4 new chimeric peptide sequences were obtained with scores above 2. Considering that the tertiary structure of the parental peptides in 75% of peptides that affect *A. baumannii* contained a helical structure, which is essentially advantageous in terms of the action mechanism, as well as ease of peptide synthesis and manipulation (40,41). Among 4 newly designed peptides only M-CIT was selected to be synthesized.

Before synthesis, M-CIT was predicted to have a hydrophobicity rate of 52%, but after synthesis, it exhibited even higher hydrophobicity and lower solubility in water due to the amino acid interactions in the peptide structure. Researchers are exploring solutions to synthesize peptides that are more cost-effective, less toxic, and have a broader range of activity. One of the most influential factors affecting these properties is the size of the peptides. Therefore, the peptide sequences were optimized for length, during which time an amino acid was removed if it either decreased or maintained the score, but retained if it increased the score. The same method was used by Lama *et al*. to design a new shortened peptide containing the active core of turbot Nkl (Nkl71-100), which was then synthesized and shown to exhibit high antiparasitic activity with a direct effect on parasite viability (42). In the last design method, which included combining amino acids based on their sequence similarity for the synthesis of the M-Pex12 peptide, after optimizing the number of amino acids and their scores it was observed that the overall secondary structure sometimes changes by removing or substituting a single amino acid at a specific position. In this study it was found that substituting arginine and valine at positions 4, 9, and 23 were highly involved in creating the maximum helical structure with the highest score.

As a small and aliphatic amino acid, the substitution of valine had a greater effect on increasing the helical structure with the appropriate score. Thus, lysine at position 4 and glycine at positions 9 and 23 in the main peptide were substituted with valine. The amino acid substitution at position 9 resulted in a more significant structural change and a higher score.

All of the results showed that certain amino acids in the peptide structure play a critical role in determining the type of peptide activity and the secondary and tertiary structures of the peptide. In a study by Zhu *et al*., threonine was replaced with tryptophan (W), which increased the hydrophobicity of the peptide and the stability of its helical structure. This led to an increase in the antibacterial activity of peptide and its potential to compete with divalent cations in the bacterial cell membrane (43). In a molecular simulation study, Raman *et al*. found that substituting alanine with valine stabilized the host peptide and its helical structure (44). Also, another study substituted the amino acids alanine, valine, and leucine in specific positions and reported increased activity of these analogues (45). In another study performed by Lee *et al*., substituting single amino acids at specific positions for piscidin-1 peptide generated new analogues of the peptide with lower cytotoxicity and increased antibacterial and anti-endotoxin activities (47). According to these studies, the above-mentioned changes increased the hydrophobicity in the peptide structure, which led to better penetration of the peptide into the bacterial membrane. The dramatic changes in peptide score associated with the removal of specific amino acids are interpreted as their key role in the peptide activity and structure.

Cationic AMPs have a major role in the potential of peptides to penetrate bacterial membranes. Both M-CIT and M-Pex12 have a net charge above 2+. Also, the peptides have a more than 50% content of alanine , isoleucine, leucine, and valine amino acids, which contribute to their stability according to the aliphatic index which represents the thermal stability of peptides. In addition, both of these peptides showed positive GRAVY indexes as well as hydrophobicity indexes above 50% in silico. M-Pex12 peptide (GRAVY index = 0.75) showed a GRAVY index of 16% more than the M-CIT peptide (GRAVY index = 0.525), which was observable in their different water solubility. Regarding the study of the helical wheel of peptides, the distribution of amino acids in both peptides was random. However, the water solubility of M-CIT was less than that of M-Pex12. In general, M-Pex12 was completely soluble in water and showed

much higher antimicrobial potency. Lee *et al*. demonstrated the key role of phenylalanine in amino acid-specific positions within the piscidin-1 peptide (46).

The results of CD analysis showed that both M-CIT and M-Pex12 displayed significantly different helical structures rather than was predicted in silico. Also, only M-Pex12 showed acceptable antimicrobial properties against the target bacterium despite that the CD analysis had shown zero helix content for it in water as a solvent. Whereas M-CIT had 5% helix content in the same conditions but did not show satisfactory antibacterial activity. MD simulation helps in understanding and describing the structural dynamic of peptides and their mechanisms of interaction with other biomolecules in atomic details. MD is also used to provide a new approach toward *de novo* protein and peptide design. Based on MD simulations, all radial distribution function analyses on M-CIT and M-Pex12 suggested that residues lysine and tyrosine directly interact with the bacterial model membranes. Tripathi *et al*. have discussed that the GXXXXG motif can effectively reduce toxicity and increase the antimicrobial potential and water solubility of a synthetic peptide (47). However, the present findings showed lower water solubility and antimicrobial properties for M-CIT containing the GXXXXG motif compared to M-Pex12 without the motif. The current study hypothesized that this inconsistency occurred due to several factors that were present in the laboratory *in vitro* conditions that might not considered during the in silico designing of the peptides.

CONCLUSION

M-CIT and M-Pex12 peptides were designed and synthesized in this study, based on bioinformatics-guided sequencing of natural peptides. The M-Pex12 peptide exhibited superior antimicrobial properties (MIC = 33.15 µM and MBC = 41.44 µM) against *A. baumannii*, while demonstrating reduced toxicity towards RBCs. In contrast, the M-CIT peptide did not exhibit significant activity against the target bacteria (MIC = 187.5 µM and MBC = 375 µM). The data presented in the current study suggested that in silico design methods can serve as useful tools for generating novel AMPs. However, several factors may potentially influence the functionality of the synthesized peptides, which can be easily overlooked during in-silico design. Therefore, it cannot be assumed that synthetic peptides will behave similarly in both simulation and laboratory studies for their physicochemical properties or biochemical function.

Acknowledgments

We would like to express our sincere gratitude to the Microbiology Research Department at Baqiyatallah University of Medical Sciences, the National Institute of Genetics of Iran, and the Office of the President for their financial support of this study. Additionally, we wish to extend our thanks to all individuals who contributed to the progress of this research. This research was financially supported by Iran National Science Foundation (INSF) (Grant No. 98027500).

Conflict of interest statement

All authors declared no conflict of interest in this study.

Authors' contributions

J. Amani and H. Mahmoodzadeh Hosseini conceptualized the study, analyzed the data and supervised the study; Y. Rakhshani performed the experimental parts of the study and wrote the manuscript; S.A. Mirhosseini and F. Sotoodeh Nejad Nematalahi did scientific editing of the manuscript. All authors approved the final version of the manuscript.

Supplementary materials

The supplementary materials for this article can be found online at: https://github.com/hosseini361/mynewsupplementary.

REFERENCES

1. Momenzadeh M, Soltani R, Shafiee F, Hakamifard A, Pourahmad M, Abbasi S. The effectiveness of colistin/levofloxacin compared to colistin/meropenem in the treatment of ventilator-associated pneumonia (VAP) caused by carbapenem-resistant *Acinetobacter baumannii*: a randomized controlled clinical trial. Res Pharm Sci. 2023;18(1):39-48. DOI: 10.4103/1735-5362.363594.

2. Ayoub Moubareck C, Hammoudi Halat D. Insights into *Acinetobacter baumannii*: a review of microbiological, virulence, and resistance traits in a threatening nosocomial pathogen. Antibiotics (Basel). 2020;9(3):119,1-29. DOI: 10.3390/antibiotics9030119.
3. Kyriakidis I, Vasileiou E, Pana ZD, Tragiannidis A. *Acinetobacter baumannii* antibiotic resistance mechanisms. Pathogens. 2021;10(3):373,1-31. DOI: 10.3390/pathogens10030373.
4. Gordon NC, Wareham DW. Multidrug-resistant *Acinetobacter baumannii*: mechanisms of virulence and resistance. Int J Antimicrob Agents. 2010;35(3):219-226. DOI: 10.1016/j.ijantimicag.2009.10.024.
5. Wang H, Guo P, Sun H, Wang H, Yang Q, Chen M, *et al*. Molecular epidemiology of clinical isolates of carbapenem-resistant *Acinetobacter* spp. from Chinese hospitals. Antimicrob Agents Chemother. 2007;51(11):4022-4028. DOI: 10.1128/AAC.01259-06.
6. Koczura R, Przyszlakowska B, Mokracka J, Kaznowski A. Class 1 integrons and antibiotic resistance of clinical *Acinetobacter calcoaceticus-baumannii* complex in Poznań, Poland. Curr Microbiol. 2014;69(3):258-262. DOI: 10.1007/s00284-014-0581-0.
7. Hancock REW, Sahl HG. Antimicrobial and host-defense peptides as new anti-infective therapeutic strategies. Nat Biotechnol. 2006;24(12):1551-1557. DOI: 10.1038/nbt1267.
8. Cotter PD, Hill C, Ross RP. Bacterial lantibiotics: strategies to improve therapeutic potential. Curr Protein Pept Sci. 2005;6(1):61-75. DOI: 10.2174/1389203053027584.
9. Lata S, Sharma BK, Raghava GPS. Analysis and prediction of antibacterial peptides. BMC Bioinform. 2007;8(1):1-10. DOI: 10.1186/1471-2105-8-263.
10. Montesinos E. Antimicrobial peptides and plant disease control. FEMS Microbiol Lett. 2007;270(1):1-11. DOI: 10.1111/j.1574-6968.2007.00683.x.
11. Ebenhan T, Gheysens O, Kruger HG, Zeevaart JR, Sathekge MM. Antimicrobial peptides: their role as infection-selective tracers for molecular imaging. Biomed Res Int. 2014;2014:867381,1-15. DOI: 10.1155/2014/867381.
12. Deslouches B, Steckbeck JD, Craigo JK, Doi Y, Mietzner TA, Montelaro RC. Rational design of engineered cationic antimicrobial peptides consisting exclusively of arginine and tryptophan, and their activity against multidrug-resistant pathogens. Antimicrob Agents Chemother. 2013;57(6):2511-2521. DOI: 10.1128/aac.02218-12.
13. Osorio D, Rondón-Villarreal P, Torres R. Peptides: a package for data mining of antimicrobial peptides. R J. 2015;7(1):4-14. DOI: 10.221RJ-2015-001/RJ-2015-001.
14. Madanchi H, Akbari S, Shabani AA, Sardari S, Farmahini Farahani Y, Ghavami G, *et al*. Alignment-based design and synthesis of new antimicrobial aurein-derived peptides with improved activity against gram-negative bacteria and evaluation of their toxicity on human cells. Drug Dev Res. 2019;80(1):162-170. DOI: 10.1002/ddr.21503.
15. Darwish R, Almaaytah A, Salama A. The design and evaluation of the antimicrobial activity of a novel conjugated penta-ultrashort antimicrobial peptide in combination with conventional antibiotics against sensitive and resistant strains of S. aureus and *E. coli*. Res Pharm Sci. 2022;17(6):612-620. DOI: 10.4103/1735-5362.359429.
16. Thandar M, Lood R, Winer BY, Deutsch DR, Euler CW, Fischetti VA. Novel engineered peptides of a phage lysin as effective antimicrobials against multidrug-resistant *Acinetobacter baumannii*. Antimicrob Agents Chemother. 2016;60(5):2671-2679. DOI: 10.1128/aac.02972-15.
17. Guo Y, Xun M, Han J. A bovine myeloid antimicrobial peptide (BMAP-28) and its analogs kill pan-drug-resistant *Acinetobacter baumannii* by interacting with outer membrane protein A (OmpA). Medicine. 2018;97(42):1-7. DOI: 10.1097/MD.0000000000012832.
18. Peng KC, Lee SH, Hour AL, Pan CY, Lee LH, Chen JY. Five different piscidins from Nile tilapia, *Oreochromis niloticus*: analysis of their expressions and biological functions. PLoS One. 2012;7(11):e50263,1-12. DOI: 10.1371/journal.pone.0050263.
19. Kim MK, Kang NH, Ko SJ, Park J, Park E, Shin DW, *et al*. Antibacterial and antibiofilm activity and mode of action of magainin 2 against drug-resistant *Acinetobacter baumannii*. Int J Mol Sci. 2018;19(10):3041,1-14. DOI: 10.3390/ijms19103041.
20. Gui S, Li R, Feng Y, Wang S. Transmission electron microscopic morphological study and flow cytometric viability assessment of *Acinetobacter baumannii* susceptible to *Musca domestica* cecropin. Sci World J. 2014;2014:657536,1-6. DOI: 10.1155/2014/657536.
21. Lee J, Jung SW, Cho AE. Molecular insights into the adsorption mechanism of human β-defensin-3 on bacterial membranes. Langmuir. 2016;32(7):1782-1790. DOI: 10.1021/acs.langmuir.5b04113.
22. Jo S, Lim JB, Klauda JB, Im W. CHARMM-GUI Membrane builder for mixed bilayers and its application to yeast membranes. Biophys J. 2009;97(1):50-58. DOI: 10.1016/j.bpj.2009.04.013.
23. Wang Y, Markwick PRL, de Oliveira CAF, McCammon JA. Enhanced lipid diffusion and mixing in accelerated molecular dynamics. J Chem Theory Comput. 2011;7(10):3199-3207. DOI: 10.1021/ct200430c.
24. Sevcsik E, Pabst G, Richter W, Danner S, Amenitsch H, Lohner K. Interaction of LL-37 with model membrane systems of different complexity: influence of the lipid matrix. Biophys J. 2008;94(12):4688-4699. DOI: 10.1529/biophysj.107.123620.

25. Cardoso P, Glossop H, Meikle TG, Aburto-Medina A, Conn CE, Sarojini V, *et al*. Molecular engineering of antimicrobial peptides: microbial targets, peptide motifs and translation opportunities. Biophys Rev. 2021;13(1):35-69. DOI: 10.1007/s12551-021-00784-y.
26. Cisneros GA, Wikfeldt KT, Ojamäe L, Lu J, Xu Y, Torabifard H, *et al*. Modeling molecular interactions in water: from pairwise to many-body potential energy functions. Chem Rev. 2016;116(13):7501-7528. DOI: 10.1021/acs.chemrev.5b00644.
27. Hess B. P-LINCS: a parallel linear constraint solver for molecular simulation. Am Chem Soc. 2008;4(1):116-122. DOI: 10.1021/ct700200b.
28. Rocklin GJ, Mobley DL, Dill KA, Hünenberger PH. Calculating the binding free energies of charged species based on explicit-solvent simulations employing lattice-sum methods: an accurate correction scheme for electrostatic finite-size effects. J Chem Phys. 2013;139(18):184103,1-32. DOI: 10.1063/1.4826261.
29. Šponer J, Bussi G, Krepl M, Banáš P, Bottaro S, Cunha RA, *et al*. RNA structural dynamics as captured by molecular simulations: a comprehensive overview. Chem Rev. 2018;118(8):4177-4338. DOI: 10.1021/acs.chemrev.7b00427.
30. Smith E. The information geometry of two-field functional integrals. Inf Geom. 2022;5(2):427-492. DOI: 10.1007/s41884-022-00071-z.
31. Idrees M, Mohammad AR, Karodia N, Rahman A. Multimodal role of amino acids in microbial control and drug development. Antibiotics (Basel). 2020;9(6): 330,1-23. DOI: 10.3390/antibiotics9060330.
32. Friedman R, Nachliel E, Gutman M. Molecular dynamics of a protein surface: ion-residues interactions. Biophys J. 2005;89(2):768-781. DOI: 10.1529/biophysj.105.058917.
33. Humphries R, Bobenchik AM, Hindler JA, Schuetz AN. Overview of changes to the clinical and laboratory standards institute performance standards for antimicrobial susceptibility testing, m100, 31st edition. J Clin Microbiol. 2021;59(12):e0021321,1-13. DOI: 10.1128/jcm.00213-21.
34. Michael A, Kelman T, Pitesky M. Overview of quantitative methodologies to understand antimicrobial resistance *via* minimum inhibitory concentration. Animals (Basel). 2020;10(8):1405,1-17. DOI: 10.3390/ani10081405.
35. Mwangi J, Yin Y, Wang G, Yang M, Li Y, Zhang Z, *et al*. The antimicrobial peptide ZY4 combats multidrug-resistant *Pseudomonas aeruginosa* and *Acinetobacter baumannii* infection. Proc Natl Acad Sci USA. 2019;116(52):26516-26522. DOI: 10.1073/pnas.1909585117.
36. Lee CM, Lai CC, Chiang HT, Lu MC, Wang LF, Tsai TL, *et al*. Presence of multidrug-resistant organisms in the residents and environments of long-term care facilities in Taiwan. J Microbiol Immunol Infect. 2017;50(2):133-144. DOI: 10.1016/j.jmii.2016.12.001.
37. Gabere MN, Noble WS. Empirical comparison of web-based antimicrobial peptide prediction tools. Bioinformatics. 2017;33(13):1921-1929. DOI: 10.1093/bioinformatics/btx081.
38. Zhang K, Teng D, Mao R, Yang N, Hao Y, Wang J. Thinking on the construction of antimicrobial peptide databases: powerful tools for the molecular design and screening. Int J Mol Sci. 2023; 24(4):1-13. DOI: 10.3390/ijms24043134.
39. Wang G, Li X, Wang Z. APD2: the updated antimicrobial peptide database and its application in peptide design. Nucleic Acids Res. 2008;37(Database issue):D933-D937. DOI: 10.1093/nar/gkn823.
40. Maccari G, Di Luca M, Nifosí R, Cardarelli F, Signore G, Boccardi C, *et al*. Antimicrobial peptides design by evolutionary multiobjective optimization. PLoS Comput Biol. 2013;9(9):e1003212,1-12. DOI: 10.1371/journal.pcbi.1003212.
41. Yamamoto N, Tamura A. Designed low amphipathic peptides with alpha-helical propensity exhibiting antimicrobial activity *via* a lipid domain formation mechanism. Peptides. 2010;31(5): 794-805. DOI: 10.1016/j.peptides.2010.01.006.
42. Lama R, Pereiro P, Costa MM, Encinar JA, Medina-Gali RM, Pérez L, *et al*. Turbot (*Scophthalmus maximus*) Nk-lysin induces protection against the pathogenic parasite *Philasterides dicentrarchi via* membrane disruption. Fish Shellfish Immunol. 2018;82:190-199. DOI: 10.1016/j.fsi.2018.08.004.
43. Zhu X, Shan A, Ma Z, Xu W, Wang J, Chou S, *et al*. Bactericidal efficiency and modes of action of the novel antimicrobial peptide T9W against *Pseudomonas aeruginosa*. Antimicrob Agents Chemother. 2015;59(6):3008-3017. DOI: 10.1128/AAC.04830-14.
44. Raman SS, Vijayaraj R, Parthasarathi R, Subramanian V. Helix forming tendency of valine substituted poly-alanine: a molecular dynamics investigation. J Phys Chem B. 2008;112(30):9100-9104. DOI: 10.1021/jp7119813.
45. de la Salud Bea R, Petraglia AF, Ascuitto MR, Buck QM. Antibacterial activity and toxicity of analogs of scorpion venom IsCT peptides. Antibiotics (Basel). 2017;6(3):13,1-8. DOI: 10.3390/antibiotics6030013.
46. Lee E, Shin A, Jeong KW, Jin B, Jnawali HN, Shin S, *et al*. Role of phenylalanine and valine10 residues in the antimicrobial activity and cytotoxicity of piscidin-1. PLoS One. 2014;9(12): e114453,1-30. DOI: 10.1371/journal.pone.0114453.
47. Tripathi AK, Kumari T, Harioudh MK, Yadav PK, Kathuria M, Shukla P, *et al.* Identification of GXXXXG motif in chrysophsin-1 and its implication in the design of analogs with cell-selective antimicrobial and anti-endotoxin activities. Sci Rep. 2017;7(1):1-16. DOI: 10.1038/s41598-017-03576-1.